TouchAnything: Diffusion-Guided 3D Reconstruction from Sparse Robot Touches

Langzhe Gu[1,3], Hung-Jui Huang[2*], Mohamad Qadri[2*], Michael Kaess[2], and Wenzhen Yuan[3†]

[1] Tsinghua University, Beijing, China
[2] Carnegie Mellon University, Pittsburgh, PA, USA
[3] University of Illinois Urbana-Champaign, Urbana, IL, USA

[*]Equal contribution [†]Corresponding author

Abstract. Accurate object geometry estimation is essential for many downstream tasks, including robotic manipulation and physical interaction. Although vision is the dominant modality for shape perception, it becomes unreliable under occlusions or challenging lighting conditions. In such scenarios, tactile sensing provides direct geometric information through physical contact. However, reconstructing global 3D geometry from sparse local touches alone is fundamentally underconstrained. We present TouchAnything, a framework that leverages a pretrained large-scale 2D vision diffusion model as a semantic and geometric prior for 3D reconstruction from sparse tactile measurements. Unlike prior work that trains category-specific reconstruction networks or learns diffusion models directly from tactile data, we transfer the geometric knowledge encoded in pretrained visual diffusion models to the tactile domain. Given sparse contact constraints and a coarse class-level description of the object, we formulate reconstruction as an optimization problem that enforces tactile consistency while guiding solutions toward shapes consistent with the diffusion prior. Our method reconstructs accurate geometries from only a few touches, outperforms existing baselines, and enables 3D reconstruction of previously unseen object instances. Our project page is `https://grange007.github.io/touchanything/`.

Keywords: Tactile Sensing · 3D Reconstruction · Generative Priors

1 Introduction

Tactile feedback is a fundamental sensory signal that enables humans to interact effectively with the physical world. Touch provides rich information about the geometry and rigidity of objects, from which the nature of possible interactions (e.g., grasps, handling) can be inferred. This becomes especially important under heavy occlusions or challenging lighting conditions, where visual perception may fail. In such situations, the ability to rely on touch alone becomes essential for estimating object geometry and enabling downstream manipulation tasks.

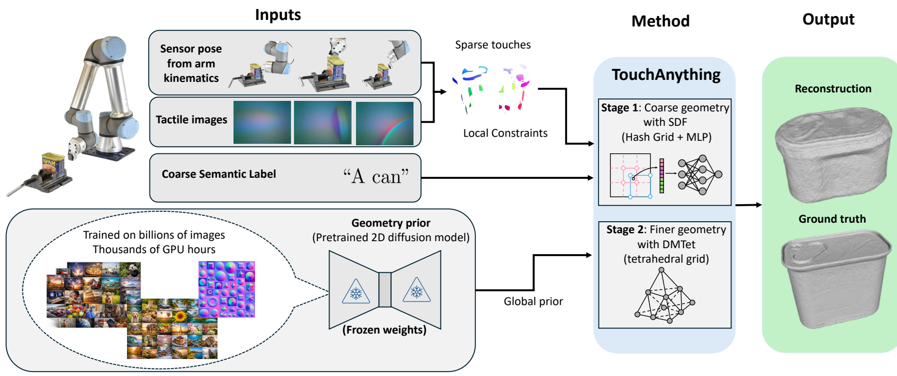

Fig. 1: Overview of TouchAnything. Sparse tactile measurements and a class-level text description are combined with a pretrained 2D diffusion model serving as a geometric prior. Local tactile constraints and global diffusion geometric guidance jointly optimize a two-stage geometric representation.

However, geometry estimation from touch alone is inherently underconstrained due to the sparsity of contact measurements. What makes this possible in humans is the presence of strong prior knowledge about object shape and structure. For example, imagine that you are tasked with finding a pen inside a backpack without visual feedback. You already possess a semantic understanding of what a "pen" typically looks like (e.g. its approximate shape and structure). As you make contact with objects inside the bag, sparse tactile cues are combined with this prior knowledge to refine your belief about the object being touched. Touch does not operate in isolation; rather, it conditions and disambiguates an existing internal model of object geometry.

This raises a natural question: can we equip robots with a similar capability? Specifically, given a robot arm equipped with tactile sensing, can we infer object geometry from sparse touches when guided by a coarse semantic prior, even when the object is previously unseen?

Recent work has demonstrated that diffusion models can serve as powerful priors for geometric reasoning. Diffusion-based approaches have been successfully applied to 3D reconstruction, text-to-3D generation, and multi-view consistent shape synthesis, enabling plausible 3D geometry inference even under limited observations or severely constrained settings. Importantly, these models are trained on large-scale visual datasets and have not been specialized to tactile signals. Nevertheless, they implicitly encode strong geometric information that may transfer across sensing modalities. To the best of our knowledge, this work is the first to adapt a general-purpose off-the-shelf pretrained 2D vision diffusion model as a geometric prior for 3D reconstruction from sparse tactile touches.

In contrast to prior touch-based reconstruction methods, which train models on class-specific datasets spanning just a handful of object categories [7, 43, 48], we develop a system that leverages the geometric priors encoded in large-scale visual diffusion models trained on billions of internet images to guide 3D reconstruction given sparse tactile measurements. We argue that transferring large-scale visual priors to the tactile domain represents an important step toward generalization to a broad category of objects, especially in regimes where tactile data is scarce and training specialized generative models is impractical.

Our contributions are as follows:

- We introduce **TouchAnything**, a framework for reconstructing global 3D object geometry from sparse tactile contacts and a coarse semantic prior, enabling 3D reconstruction for a large category of objects from limited physical interaction.
- We demonstrate that large-scale pretrained 2D vision diffusion models can be repurposed as geometric priors for tactile reconstruction, transferring visual generative knowledge to the tactile domain without task-specific diffusion training.
- We provide extensive validation in simulation and real-world robotic experiments, including a study of reconstruction accuracy under varying numbers of touches and prompt designs.

2 Related Work

2.1 3D Reconstruction from Sparse Observations

Neural implicit and differentiable geometric representations such as neural radiance fields (NeRF) [19], signed distance fields (SDFs) [22,41], hybrid mesh-based approaches like DMTet [35], and more recently 3D Gaussian Splatting [14], have become dominant frameworks for 3D reconstruction. These methods introduce differentiable parameterizations of geometry and appearance, making them well-suited for end-to-end optimization. Beyond RGB-based reconstruction, their flexibility has enabled applications across diverse sensing modalities [15,18,24,27,29,30,49], including tactile sensing [7,37]. However, regardless of the underlying representation or sensing modality, 3D reconstruction becomes severely underconstrained when observations provide only limited geometric coverage of the underlying surface [21,40]. In few-view settings, implicit and differentiable models alone are insufficient to solve for global geometry without additional regularization. This challenge is further amplified in tactile reconstruction, where measurements come from small local contact patches rather than partial global image observations.

2.2 Diffusion Models as Geometric Priors

Recent advances in diffusion modeling have demonstrated that large-scale generative models implicitly encode rich knowledge about object geometry. DreamFusion [23] introduced the use of pretrained 2D text-to-image diffusion models to optimize 3D representations via score distillation sampling (SDS), enabling text-to-3D generation without direct 3D supervision. Subsequent works [17, 28, 44], improved fidelity and enhanced geometric detail in diffusion-guided 3D synthesis. Fantasia3D [5] and RichDreamer [28] explicitly incorporate geometric signals such as surface normals and depth to better disentangle shape and appearance during diffusion-guided 3D generation. These works demonstrate that diffusion models can effectively leverage explicit geometric cues to improve the quality of the generated geometry. In our setting, we similarly render normal maps from the evolving 3D geometry. However, unlike prior methods, we additionally enforce consistency with real local surface normal measurements obtained from image-based tactile sensors. We therefore combine global diffusion guidance with physical local constraints imposed by robot contact. Tactile DreamFusion [10] similarly incorporates tactile signals into text-to-3D synthesis, but its primary objective remains asset generation, whereas our goal is tactile-conditioned 3D reconstruction constrained by real tactile measurements.

Beyond text-to-3D synthesis, sparse 3D reconstruction has been addressed by learning task-specific shape completion priors from curated 3D datasets [6, 46]. More recently, diffusion-based completion models [34] train 3D diffusion priors to regularize underconstrained geometric inference and recover plausible structure from partial observations. Unlike these approaches, which require supervised training on 3D shape collections, we leverage a pretrained 2D diffusion model as a transferable geometric prior without task-specific diffusion training.

Several recent works [13, 20, 45, 51] also employ diffusion models as geometric priors for sparse-view 3D reconstruction from RGB images or partial point clouds, where diffusion guidance regularizes geometry estimated from limited visual coverage. In contrast, our setting relies solely on sparse local tactile contacts, which provide highly localized surface measurements without global image-level constraints. Inferring global geometry from such physical interaction signals is a different and a more severely underconstrained problem.

2.3 Tactile-based Shape Reconstruction

Image-based tactile sensors provide useful geometric information (e.g. contact location and surface normals) which have been leveraged for object state estimation and tracking during interaction [11, 12, 25, 26] as well as 3D reconstruction. TouchSDF [7] predicts local surface geometry from vision-based tactile sensors and learns an SDF encoding the object shape. More recently, diffusion-based tactile reconstruction methods [43, 48] train conditional diffusion models for tactile-conditioned 3D reconstruction using object-level datasets such as ShapeNet and ABC. These approaches rely on supervised training with ground-truth 3D geometry from fixed object categories (e.g., guitars, bottles), which may limit generalization beyond seen categories and involve computationally intensive task-specific training of diffusion models. Other works [8, 9, 37–39] fuse tactile and visual measurements for 3D reconstruction benefiting from the global visual coverage provided by vision. However, they differ from our setting where

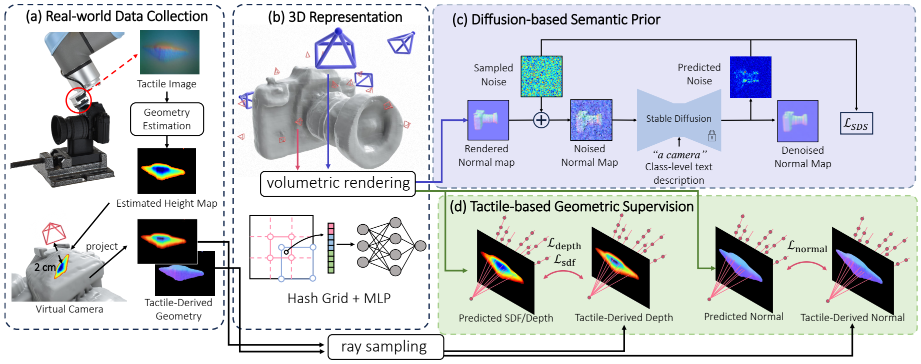

Fig. 2: TouchAnything reconstruction pipeline. We use a GelSight tactile sensor mounted on a robotic arm to collect raw tactile measurements, which are converted into local depth and surface normal maps (Sec. 3.1). These measurements provide sparse geometric supervision for learning a neural signed distance field (SDF) by enforcing local constraints through depth and normal losses. Normal maps rendered from the evolving 3D geometry are fed into a pretrained Stable Diffusion model, which provides global geometric guidance through score distillation sampling (SDS). By jointly enforcing tactile consistency combined with a pretrained 2D diffusion model and a class-level text description, the system reconstructs globally consistent 3D geometry from sparse contact measurements (Sec. 3.2).

touch provides the primary geometric signal. Overall, prior tactile reconstruction methods either depend on dense measurements, multi-modal sensing, or expensive training of task-specific generative priors. To the best of our knowledge, reconstructing global object geometry from sparse tactile contacts using pretrained off-the-shelf 2D diffusion models remains unexplored.

3 Methodology

Our goal is to reconstruct the 3D geometry of a previously unseen object using only sparse tactile readings and a minimal class-level text description (e.g. "a camera", "a bottle"). We assume that the contact locations of tactile readings are known from robot kinematics. The text description provides only a weak semantic prior at the category level, reflecting realistic scenarios where a robot knows the object class but not the specific geometry, such as searching for a key in the wallet.

To solve this problem, we propose TouchAnything, a diffusion-guided method for 3D reconstruction from sparse tactile inputs. Instead of utilizing a model trained on limited object categories [7, 48], we leverage Stable Diffusion [32], a general-purpose generative model, to guide reconstruction, conditioned on the weak text description. This design makes our method much more general, enabling reconstruction of previously unseen objects without pre-training or class-specific data collection. In TouchAnything, tactile readings are first converted into local depth maps using established methods [38, 42], and are represented as virtual camera observations to ensure compatibility with the vision-centric reconstruction pipeline. We then adopt a coarse-to-fine reconstruction strategy inspired by Magic3D [17] and optimize the object geometry by jointly enforcing consistency with tactile-derived geometry and alignment with the class-level text description.

3.1 Deriving Local Geometry from Tactile Sensing

We use a GelSight sensor [47] to collect tactile data. GelSight is a vision-based tactile sensor composed of a soft elastomer sensing surface, an integrated illumination system, and a camera. Upon contact, the elastomer deforms, changing the reflected illumination pattern, which is captured by the camera and used to reconstruct the contact surface geometry via photometric stereo. A sample tactile image is shown in Fig. 2a. In our work, GelSight images are obtained from both real-world experiments and simulations. From these images, we estimate the local contact geometry and convert it into virtual camera observations for compatibility with the vision-centric reconstruction pipeline.

Geometry Estimation from Real-World Tactile Data Given a tactile image $\mathbf{T}$ collected by a physical GelSight sensor, we adopt the learning-based method in [42] to estimate per-pixel surface gradients from the RGB values and coordinates of each pixel using a three-layer MLP. The predicted gradients are then integrated using a fast Poisson solver [47] to recover the surface depth map. The contact mask is obtained by thresholding the estimated depth map.

Geometry Estimation from Simulated Tactile Data Given a photorealistic simulated GelSight image, we adopt the learning-based method in [38], using a multi-head U-Net [33] to jointly predict the depth map and contact mask. The network is trained on 20k simulated GelSight images generated from contacts with 78 YCB objects [3]. Compared to the real-world scenario, we use a more complex geometry estimation model for simulated tactile data because larger-scale training data are available in simulation.

Tactile-Derived Geometry as Virtual Camera Observation For each tactile reading $\mathbf{T}_i$, we place a virtual camera $\mathbf{C}_i$ 2.0 cm behind the contact patch and convert the tactile-estimated depth map and contact mask into virtual camera observations consisting of depth and normal maps with an associated contact mask. The reconstruction process then operates on these tactile-derived geometries in the form of virtual camera observations rather than the raw tactile readings, ensuring compatibility with the vision-centric reconstruction pipeline. The full data collection pipeline is shown in Fig. 2a.

3.2 Stage 1: Learning Coarse Geometry of the Object

We model the coarse object geometry using a SDF-based neural implicit representation $f_\theta : \mathbb{R}^3 \to \mathbb{R}$, implemented using a Neuralangelo-style [16] multi-resolution 3D hash-grid features followed by an MLP (Fig. 2b). The function f_θ maps a 3D coordinate to its truncated signed distance to the object surface, and its zero level set defines the reconstructed shape. We optimize θ by minimizing a joint objective that enforces geometric consistency with the tactile-derived geometry while encouraging semantic consistency through a diffusion-based prior on the class-level text description.

Tactile-based Geometric Supervision Consider reconstructing an object that is touched K times at different locations, producing tactile readings $\mathbf{T}_1, ..., \mathbf{T}_K$. As described in Sec. 3.1, we convert each tactile reading into a virtual camera observation consisting of depth maps, normal maps, and contact regions. We use these observations to impose sparse geometric constraints on the object surface represented by the SDF function f_θ. However, to impose these constraints, we need to first represent the virtual camera observations in a ray-based form compatible with our reconstruction algorithm (Fig. 2d).

Let $\mathcal{R}$ denote the union of all rays cast from the K virtual cameras $\{\mathbf{C}_K\}$, where each ray originates from a virtual camera center and passes through a pixel within the contacted region. For each ray $r \in \mathcal{R}$, the tactile-derived depth and normal maps in the virtual camera frame provide the depth observation $d(r)$ and surface normal observation $\mathbf{n}(r)$ along that ray.

To enforce geometric constraints from the tactile-derived ray observations $d(r)$ and $\mathbf{n}(r)$, we adopt the volumetric rendering formulation of Neuralangelo [16]. For each ray $r \in \mathcal{R}$, we use the SDF function f_θ along the ray to compute the predicted depth $d_\theta(r)$ and surface normal $\mathbf{n}_\theta(r)$. These computed quantities are differentiable with respect to the SDF parameters θ, allowing us to enforce geometric consistency by minimizing the discrepancy between the SDF-computed depth and normal values and the tactile-derived depth and normal values:

$$\mathcal{L}_{\text{depth}} = \mathbb{E}_{r\sim\mathcal{R}}\left[|d(r) - d_\theta(r)|\right], \qquad \mathcal{L}_{\text{normal}} = \mathbb{E}_{r\sim\mathcal{R}}\left[\|\mathbf{n}(r) - \mathbf{n}_\theta(r)\|_1\right] \quad (1)$$

Beyond supervision on these computed quantities, we incorporate two additional supervision signals following [1]. The first supervises the signed distance values near the observed surface, and the second enforces freespace constraints along the ray up to the surface. To supervise the SDF, for each ray r with a tactile-derived depth observation $d(r)$, we sample depths s within a truncated band $\mathcal{S}_r^{\text{sdf}} = [d(r) - \delta,\ d(r) + \delta]$ around the surface, where δ denotes the truncation distance. Let $\mathbf{x}(r, s)$ denote the 3D point at depth s along ray r, the SDF loss is:

$$\mathcal{L}_{\text{sdf}} = \mathbb{E}_{r\sim\mathcal{R}}\ \mathbb{E}_{s\sim\mathcal{S}_r^{\text{sdf}}}\left|f_\theta(\mathbf{x}(r,s)) - (s - d(r))\right|. \quad (2)$$

To enforce freespace constraints, we additionally sample points in $\mathcal{S}_r^{\text{fs}} = [0,\ d(r) - \delta]$, which extends from the virtual camera center to a distance δ before the surface. Since this region should be physically occupied by the tactile sensor and should remain free of objects, we penalize the predicted signed distance to be smaller than the distance δ:

$$\mathcal{L}_{\text{fs}} = \mathbb{E}_{r\sim\mathcal{R}}\ \mathbb{E}_{s\sim\mathcal{S}_r^{\text{fs}}}\left[\text{ReLU}(\delta - f_\theta(\mathbf{x}(r,s)))^2\right]. \tag{3}$$

We optimize a weighted combination of these four losses to enforce geometrical consistency with the tactile observations. In practice, the expected values of the losses are estimated by sampling a batch of rays $r \in \mathcal{R}$ during each training iteration.

Diffusion-based Prior To guide the reconstructed geometry to align with the class-level text description (e.g. "a camera"), we incorporate a diffusion prior. In particular, we use Stable Diffusion [32], a general-purpose generative model, and apply score distillation sampling (SDS) [23] to impose geometric and semantic guidance during optimization (Fig. 2c).

At each optimization step, we uniformly sample a virtual camera pose from a sphere centered at the object and render a surface normal image $\mathbf{N}_\theta$ via volumetric rendering of the SDF f_θ. Following Fantasia3D [5], we supervise the geometry using the normal map rather than an RGB image to focus on providing fine surface details. We denote $\mathbf{z}(\mathbf{N}_\theta)$ as the latent feature obtained by passing the rendered normal map $\mathbf{N}_\theta$ through the Stable Diffusion VAE encoder. The SDS gradient with respect to the SDF parameters θ is:

$$\nabla_\theta \mathcal{L}_{\text{SDS}} = \mathbb{E}_{t,\epsilon}\left[w(t)\big(\hat{\epsilon}_\phi(\mathbf{z}_t(\mathbf{N}_\theta); y, t) - \epsilon\big)\frac{\partial \mathbf{z}(\mathbf{N}_\theta)}{\partial \theta}\right] \tag{4}$$

where $\hat{\epsilon}_\phi$ is the noise predicted by Stable Diffusion, y is the text description, and ϵ is the actual noise added to the latent $\mathbf{z}$ to produce the noisy version $\mathbf{z}_t$. Additionally, t denotes the diffusion timestep, and $w(t)$ is a timestep-dependent weighting function. By backpropagating this SDS gradient, we refine the SDF parameters θ, so the reconstructed geometry matches the text description y.

Training Schedule The final optimization objective combines the tactile-defined geometric losses (Eq. (1), Eq. (2), and Eq. (3)), the diffusion-guided SDS loss (Eq. (4)), and the Eikonal regularization term. We adopt a two-stage training strategy. In the warm-up stage (steps 0–1000), optimization is driven only by tactile supervision to establish a geometry consistent with the tactile readings. In the joint refinement stage (steps 1000-7000), we optimize the model with both tactile supervision and SDS guidance, where the diffusion model operates on 64×64 rendered normal images with a batch size of 8.

3.3 Stage 2: Learning Fine Geometry of the Object

To refine geometric details beyond the coarse reconstruction, we further learn fine object geometry using DMTet, an explicit tetrahedral-grid SDF representation. In Sec. 3.2, the diffusion-based prior is constrained to apply to low-resolution rendered images of 64×64, because the underlying geometry is represented by an MLP that predicts SDF values and requires expensive per-ray field queries for volumetric rendering. Rendering at higher resolutions is therefore computationally prohibitive, which limits the diffusion prior's ability to recover fine geometric details. In contrast, DMTet adopts a fully explicit representation. It discretizes the signed distance field onto a tetrahedral grid with vertices $\mathcal{V} = \{v_i\}_{i=1}^{N_v}$ and parameterizes the geometry by per-vertex signed distance values $\{s_i\}_{i=1}^{N_v}$ and per-vertex offsets $\{\Delta v_i\}_{i=1}^{N_v}$, where N_v is the number of grid vertices. This representation eliminates the need for MLP evaluation and per-ray field queries. The object surface can be extracted using differentiable marching tetrahedra and rendered with differentiable rasterization, which is significantly more efficient than rendering with the Neuralangelo-style SDF representation used in Sec. 3.2. Consequently, DMTet enables rendering at a much higher resolution of 512×512 with batch size 4.

Let $\phi = \{\{s_i\}, \{\Delta v_i\}\}$ denote the learnable parameters of DMTet. We initialize s_i by querying the SDF of the optimized coarse geometry from Sec. 3.2 at each grid vertex. Similar to learning the coarse geometry, we optimize ϕ by minimizing the weighted sum of the depth loss $\mathcal{L}_{\text{depth}}$, normal loss $\mathcal{L}_{\text{normal}}$, and the SDS loss $\mathcal{L}_{\text{SDS}}$. Different from stage 1, these losses are now computed through efficient differentiable rasterization instead of ray casting and MLP evaluation. In particular, the SDS loss is evaluated at a much higher rendering resolution, enabling the diffusion-based prior to recover finer geometric details. Beyond these losses, we additionally include the normal consistency loss [31] that penalizes angular deviations between adjacent vertex normals, encouraging locally smooth surface geometry:

$$\mathcal{L}_{\text{nc}} = \frac{1}{|\mathcal{E}|} \sum_{(i,j)\in\mathcal{E}} \left(1 - \cos(\mathbf{n}_i, \mathbf{n}_j)\right), \tag{5}$$

where $\mathcal{E}$ denotes the set of mesh edges, and $\mathbf{n}_i$ and $\mathbf{n}_j$ are the unit vertex normals at the endpoints of edge (i, j). More details about fine geometry learning are provided in the Supplementary Material.

4 Experiments and Results

We evaluate the reconstruction performance of TouchAnything in simulation and compare it with baseline methods. We additionally demonstrate its qualitative performance in real-world scenarios and conduct ablation studies to examine the impact of different modality inputs. All objects were trained on a single NVIDIA A100 GPU which takes ~ 1 hour for stage 1 and 40 minutes for stage 2.

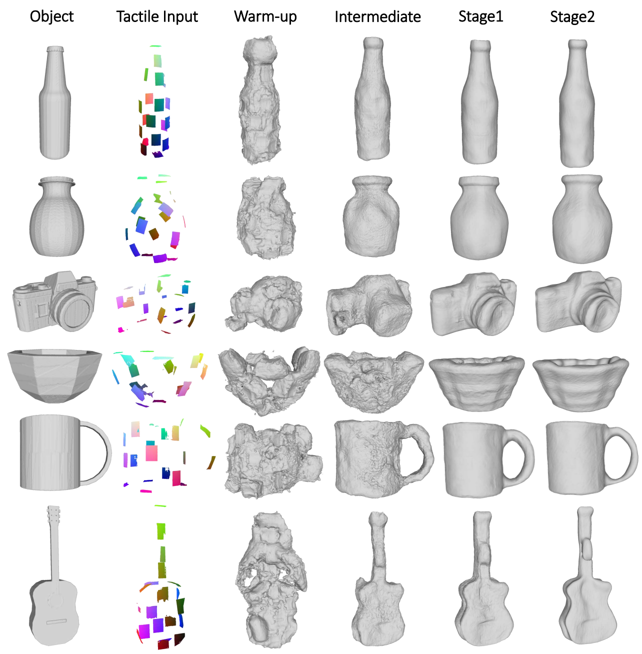

Fig. 3: Visualization of the simulation results. From left to right, we show the ground truth object, the tactile measurements, the result from the warm-up stage where only tactile observations are used, followed by intermediate, stage 1, and stage 2 reconstructions. The warm-up stage provides a good initialization of the shape before incorporating the diffusion model. We also note that the stage 1 results are close to stage 2 because the simulated objects contain limited geometric detail.

4.1 Simulation Experiments

Data Collection We evaluate TouchAnything on 280 objects from ShapeNetCore.V2 [4]. We use the same object subset as TouchSDF [7], provided by its authors, to enable direct comparison with it and subsequent work [43]. The objects span six categories: bowls, bottles, cameras, jars, guitars, and mugs. The class-level text prompt associated with each category is defined respectively as "a bowl", "a bottle", "a camera", "a jar", "a guitar", and "a mug". For each object, we generate 20 simulated tactile images as input to TouchAnything. This is achieved through a tactile simulation pipeline designed to closely approximate how a robot interacts with objects in real-world scenarios. We use Taxim [36], an example-based photorealistic tactile simulator, to produce GelSight images. For each object mesh, we uniformly sample contact locations (see Supplementary Material for details), align the contact orientation with the local surface normal, and press the object to a predefined depth. Open3D ray casting [50] is then used to compute the resulting contact depth map, which Taxim converts into a photorealistic GelSight image with a resolution of 320×240 corresponding to a sensing area of 2.0cm $\times$ 1.5cm.

Baseline Methods We compare our approach to two tactile-based 3D reconstruction methods. **TouchSDF** [7] reconstructs 3D geometry using TacTip tactile sensors and is a common baseline in tactile-based 3D reconstruction research. It represents object geometry using DeepSDF, a neural implicit representation pretrained on a specific dataset, which provides a dataset-specific shape prior during reconstruction. **Touch2Shape** [43] uses an active tactile exploration strategy and additionally trains a diffusion model on tactile data to provide a generative shape prior during reconstruction. In contrast, our approach uses a general-purpose model guided only by minimal text descriptions, enabling reconstruction for a broad category of objects without dataset-specific training.

Table 1: Quantitative Results on the simulation data. We show the Earth Mover's Distance (EMD) metric for various methods on test objects with 20 robot touches.

Category	TouchSDF [7]	Touch2Shape [43]	Ours
Bottle	0.047 ± 0.024	0.041	$\mathbf{0.035} \pm 0.020$
Bowl	0.048 ± 0.017	0.049	$\mathbf{0.039} \pm 0.010$
Camera	0.092 ± 0.043	0.056	$\mathbf{0.047} \pm 0.025$
Guitar	0.155 ± 0.087	0.064	$\mathbf{0.060} \pm 0.025$
Jar	0.071 ± 0.038	0.055	$\mathbf{0.053} \pm 0.023$
Mug	0.066 ± 0.018	0.049	$\mathbf{0.044} \pm 0.008$

Experimental Results We evaluate the reconstruction results using Earth Mover's Distance (EMD), which is widely used in touch-based reconstruction and better reflects visual quality [7]. The result is reported in Tab. 1. TouchAnything achieves better reconstruction performance across all categories compared to both baselines, highlighting our method's ability to leverage the rich geometric priors encoded in off-the-shelf 2D diffusion models. In Fig. 3, we show sample results from the warmup, stage 1 and stage 2. We note that the warmup stage provides a good initialization of the geometry before further refinement with the diffusion prior while the later incorporation of the diffusion model further improves the reconstruction quality.

4.2 Real-world Experiments with a Robot

Hardware The real-world experiments are conducted with a 6-DOF UR5e robot arm equipped with a Gelsight Mini tactile sensor. The sensor operates at a resolution of 320×240, corresponding to a sensing area of 2.0cm $\times$ 1.5cm. For real-world evaluation, we selected 14 objects in total, including 6 objects selected from the YCB dataset, 3 3D-printed objects chosen from ShapeNetCore.V2 [4] and 5 household objects. The 3D-printed objects were designed to be mounted on a cuboid base. During the experiments, all objects were rigidly fixed to the table using a dedicated mount.

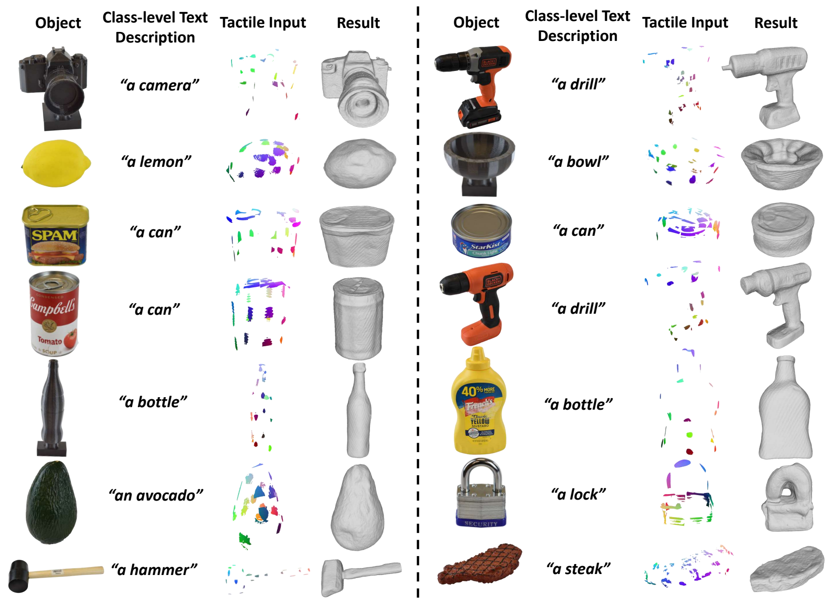

Fig. 4: Real-world reconstruction results with TouchAnything. For each object, we show the class-level text description, an image of the real object, and the 20 tactile measurements used for reconstruction. The rightmost column shows the results obtained from stage 2.

Data Collection We collected the real-world data by operating the robot arm to make contact with the object. The contact poses were selected to best cover the surface of the object uniformly. A GelSight image is collected after every touch, and the pose of the sensor is calculated using the forward kinematics of the robot arm. Additionally, considering real robot interactions may naturally produce non-uniform tactile observations due to reachability and graspability constraints, we further evaluate non-uniform touch distributions in the Supplementary Material, including contacts biased toward graspable regions and contacts concentrated on one side of the object.

Experimental Results Fig. 4 presents the tactile input and reconstruction results for all real-world objects. For each object, 20 touches are applied uniformly across the surface. Despite the sparse tactile observations, TouchAnything achieves good reconstruction of the object geometry. For complex objects such as the camera and drill, large portions of the object remain untouched. Nevertheless, our diffusion prior correctly completes these regions with detailed shapes consistent with the semantic description. More importantly, as shown in Fig. 4, our method successfully reconstructs all tested real-world objects. This is possible because we use a general-purpose generative model rather than dataset-specific models. In contrast, prior methods [7,43,48] can typically reconstruct only objects from categories seen during training which highlights the stronger generalization capability of our approach. Fig. 5 shows the fine geometric details recovered during the stage 2 refinement step compared to the coarse geometry obtained in stage 1. Additional qualitative results are available in the Supplementary Material.

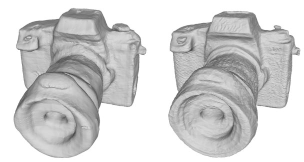

Fig. 5: Stage 1 results on the left and stage 2 result on the right. Note the finer details recovered via the refinement step.

4.3 Ablation Studies

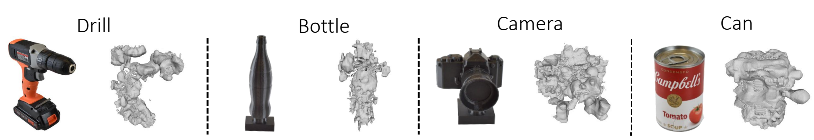

Fig. 6: Reconstructions using only tactile observations after removing the diffusion prior. The reconstructions degrade significantly.

Ablation: Tactile-Only Reconstruction. Fig. 6 shows 3D reconstructions of real objects obtained using tactile observations only, after removing the diffusion prior. The reconstruction quality degrades significantly compared to our full method, highlighting the importance of the diffusion model. This behavior is expected, as tactile sensing provides only local geometric measurements. With a limited number of touches, the reconstruction problem remains highly underconstrained without the global guidance provided by the diffusion prior.

Ablation: Text Description and Touch Count. We study how the number of touches and the quality of text description affect the reconstruction performance of TouchAnything. To evaluate the effect of additional tactile supervision, we run TouchAnything using 20, 40, and all available touches. We also investigate the effect of semantic guidance by varying the text description provided to the model. Specifically, we consider four levels of semantic text guidance: an incorrect description (e.g., "an airplane"), no description (an empty string), a class-level description (e.g., "a camera"), and a highly detailed instance-specific description. Fig. 7 shows the reconstruction results of TouchAnything under different input combinations on four real-world objects: a camera, drill, cola bottle, and tomato soup can. With only 20 tactile observations, we show that a class-level text description (e.g., "a camera") is sufficient for TouchAnything to

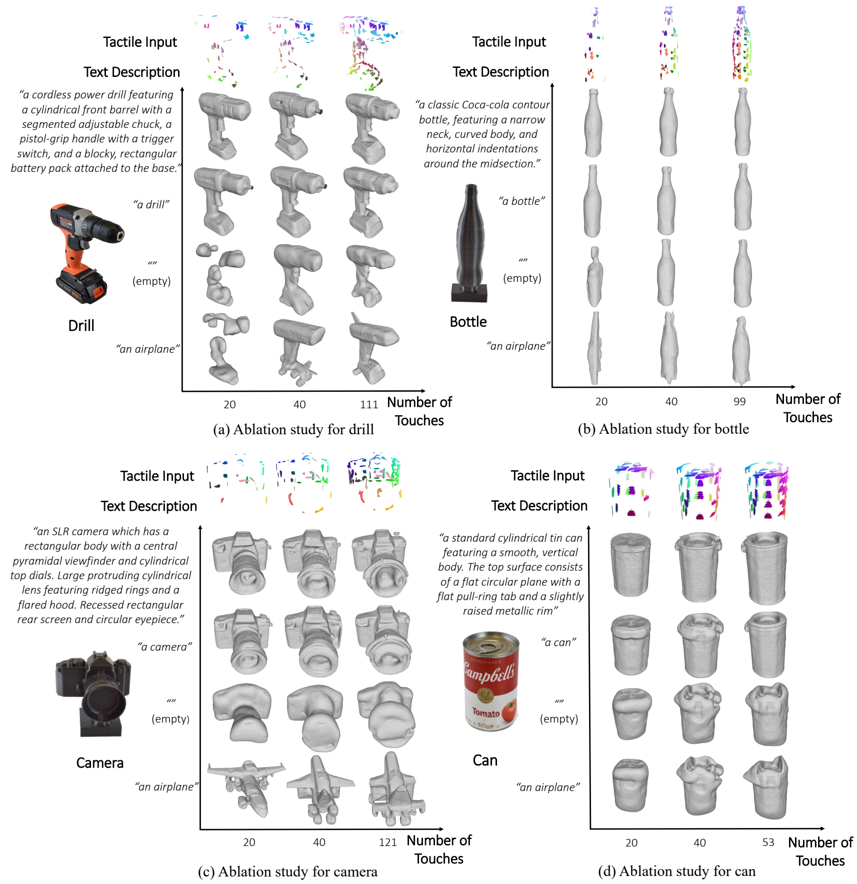

(a) Ablation study for drill (b) Ablation study for bottle (c) Ablation study for camera (d) Ablation study for can

Fig. 7: We study the effect of the number of tactile measurements and the text description used to guide the diffusion prior on reconstruction quality. Columns correspond to increasing numbers of touches, while rows correspond to different text descriptions (detailed, class-level, empty, and incorrect). Our method reconstructs plausible geometries with as few as 20 touches while more informative descriptions guide the reconstruction toward more realistic shapes.

correctly complete the untouched regions, and a more detailed description does not necessarily improve reconstruction as precise geometric details are hard to specify through text. The influence of the diffusion prior is further illustrated when an incorrect description, such as "an airplane," is used, which causes the model to hallucinate structures in the unseen regions that match the incorrect semantics. Even when using an empty string as the text description, we show that the diffusion model can still reasonably infer unseen geometry based on common-sense geometric reasoning, such as connecting aligned surface patches or completing partial cylindrical structures. For completeness, we include the quantitative results (EMD) of TouchAnything under different input combinations for four real-world objects with ground-truth meshes in the Supplementary Material.

5 Discussion and Conclusion

We present TouchAnything, a method for reconstructing 3D object geometry from sparse tactile measurements by leveraging an off-the-shelf pretrained 2D diffusion model as a semantic and geometric prior. Our approach combines local geometric constraints derived from tactile sensing with global guidance from a diffusion prior for 3D reconstruction. As a result, it addresses the fundamentally underconstrained nature of reconstructing shapes from sparse physical contacts. Unlike prior tactile reconstruction methods that rely on category-specific training or diffusion models trained directly on tactile datasets, TouchAnything transfers geometric knowledge encoded in large-scale visual diffusion models to the tactile domain. Our results demonstrate that this combination enables accurate and robust 3D reconstruction from only a small number of touches while generalizing to previously unseen objects. Several promising directions remain for future work. One direction is to investigate the possibility of removing the reliance on text prompts entirely, enabling fully prompt-free reconstruction from tactile measurements. Additionally, our current system assumes that tactile measurements are collected passively. Future work could explore active touch strategies that guide the robot toward the most informative contact locations, enabling more efficient data collection and reconstruction.

Acknowledgements

The authors thank Ruohan Zhang and Jingyi Xiang for their help with robot setup and hardware design, thank Ruihan Gao for her discussions on tactile-inspired 3D generation, and thank Yuchen Mo for the support with computing resources. Mohamad Qadri was supported in part by ONR grant N00014-24-1-2272. This work used the Delta system at the National Center for Supercomputing Applications [award OAC 2005572] through allocation CIS240782 from the Advanced Cyberinfrastructure Coordination Ecosystem: Services & Support (ACCESS) program [2], which is supported by National Science Foundation grants #2138259, #2138286, #2138307, #2137603, and #2138296.

References

1. Azinović, D., Martin-Brualla, R., Goldman, D.B., Nießner, M., Thies, J.: Neural rgb-d surface reconstruction. In: Proceedings of the IEEE/CVF Conference on Computer Vision and Pattern Recognition (CVPR). pp. 6290–6301 (June 2022)
2. Boerner, T.J., Deems, S., Furlani, T.R., Knuth, S.L., Towns, J.: ACCESS: Advancing Innovation: NSF's Advanced Cyberinfrastructure Coordination Ecosystem: Services & Support. In: Practice and Experience in Advanced Research Computing (PEARC '23). p. 4. ACM, Portland, OR, USA (July 2023). `https://doi.org/10.1145/3569951.3597559`

3. Calli, B., Singh, A., Bruce, J., Walsman, A., Konolige, K., Srinivasa, S., Abbeel, P., Dollar, A.M.: Yale-cmu-berkeley dataset for robotic manipulation research. The International Journal of Robotics Research **36**(3), 261–268 (2017). https://doi.org/10.1177/0278364917700714
4. Chang, A.X., Funkhouser, T., Guibas, L., Hanrahan, P., Huang, Q., Li, Z., Savarese, S., Savva, M., Song, S., Su, H., Xiao, J., Yi, L., Yu, F.: ShapeNet: An Information-Rich 3D Model Repository. Tech. Rep. arXiv:1512.03012 [cs.GR], Stanford University — Princeton University — Toyota Technological Institute at Chicago (2015)
5. Chen, R., Chen, Y., Jiao, N., Jia, K.: Fantasia3d: Disentangling geometry and appearance for high-quality text-to-3d content creation. In: Proceedings of the IEEE/CVF international conference on computer vision. pp. 22246–22256 (2023)
6. Chibane, J., Pons-Moll, G.: Implicit feature networks for texture completion from partial 3d data. In: European Conference on Computer Vision. pp. 717–725. Springer (2020)
7. Comi, M., Lin, Y., Church, A., Tonioni, A., Aitchison, L., Lepora, N.F.: Touchsdf: A deepsdf approach for 3d shape reconstruction using vision-based tactile sensing. IEEE Robotics and Automation Letters **9**(6), 5719–5726 (2024)
8. Comi, M., Tonioni, A., Tremblay, J., Yang, M., Blukis, V., Lin, Y., Lepora, N.F., Aitchison, L.: Snap-it, tap-it, splat-it: Tactile-informed 3d gaussian splatting for reconstructing challenging surfaces. In: 2025 International Conference on 3D Vision (3DV). pp. 1134–1143. IEEE (2025)
9. Fang, I., Shi, K., He, X., Tan, S., Wang, Y., Zhao, H., Huang, H.J., Yuan, W., Feng, C., Zhang, J.: Fusionsense: Bridging common sense, vision, and touch for robust sparse-view reconstruction. In: 2025 IEEE International Conference on Robotics and Automation (ICRA). pp. 15798–15805. IEEE (2025)
10. Gao, R., Deng, K., Yang, G., Yuan, W., Zhu, J.Y.: Tactile dreamfusion: Exploiting tactile sensing for 3d generation. Advances in Neural Information Processing Systems **37**, 29839–29863 (2024)
11. Huang, H.J., Kaess, M., Yuan, W.: Normalflow: Fast, robust, and accurate contact-based object 6dof pose tracking with vision-based tactile sensors. IEEE Robotics and Automation Letters (2024)
12. Huang, H.J., Mirzaee, M.A., Kaess, M., Yuan, W.: Gelslam: A real-time, high-fidelity, and robust 3d tactile slam system. arXiv preprint arXiv:2508.15990 (2025)
13. Kasten, Y., Rahamim, O., Chechik, G.: Point cloud completion with pretrained text-to-image diffusion models. Advances in Neural Information Processing Systems **36**, 12171–12191 (2023)
14. Kerbl, B., Kopanas, G., Leimkühler, T., Drettakis, G., et al.: 3d gaussian splatting for real-time radiance field rendering. ACM Trans. Graph. **42**(4), 139–1 (2023)
15. Kung, P.C., Harisha, S., Vasudevan, R., Eid, A., Skinner, K.A.: Radarsplat: Radar gaussian splatting for high-fidelity data synthesis and 3d reconstruction of autonomous driving scenes. In: Proceedings of the IEEE/CVF International Conference on Computer Vision. pp. 27596–27606 (2025)
16. Li, Z., Müller, T., Evans, A., Taylor, R.H., Unberath, M., Liu, M.Y., Lin, C.H.: Neuralangelo: High-fidelity neural surface reconstruction. In: IEEE Conference on Computer Vision and Pattern Recognition (CVPR) (2023)
17. Lin, C.H., Gao, J., Tang, L., Takikawa, T., Zeng, X., Huang, X., Kreis, K., Fidler, S., Liu, M.Y., Lin, T.Y.: Magic3d: High-resolution text-to-3d content creation. In: Proceedings of the IEEE/CVF conference on computer vision and pattern recognition. pp. 300–309 (2023)

18. Lin, T., Qadri, M., Zhang, K., Pediredla, A., Metzler, C.A., Kaess, M.: Acoustic neural 3d reconstruction under pose drift. In: 2025 IEEE/RSJ International Conference on Intelligent Robots and Systems (IROS). pp. 12704–12711. IEEE (2025)
19. Mildenhall, B., Srinivasan, P.P., Tancik, M., Barron, J.T., Ramamoorthi, R., Ng, R.: Nerf: Representing scenes as neural radiance fields for view synthesis. Communications of the ACM **65**(1), 99–106 (2021)
20. Ni, J., Liu, Y., Lu, R., Zhou, Z., Zhu, S.C., Chen, Y., Huang, S.: Decompositional neural scene reconstruction with generative diffusion prior. In: Proceedings of the IEEE/CVF Conference on Computer Vision and Pattern Recognition (CVPR). pp. 6022–6033 (June 2025)
21. Niemeyer, M., Barron, J.T., Mildenhall, B., Sajjadi, M.S., Geiger, A., Radwan, N.: Regnerf: Regularizing neural radiance fields for view synthesis from sparse inputs. In: Proceedings of the IEEE/CVF conference on computer vision and pattern recognition. pp. 5480–5490 (2022)
22. Park, J.J., Florence, P., Straub, J., Newcombe, R., Lovegrove, S.: Deepsdf: Learning continuous signed distance functions for shape representation. In: Proceedings of the IEEE/CVF conference on computer vision and pattern recognition. pp. 165–174 (2019)
23. Poole, B., Jain, A., Barron, J.T., Mildenhall, B.: Dreamfusion: Text-to-3d using 2d diffusion. arXiv preprint arXiv:2209.14988 (2022)
24. Qadri, M., Kaess, M., Gkioulekas, I.: Neural implicit surface reconstruction using imaging sonar. In: 2023 IEEE International Conference on Robotics and Automation (ICRA). pp. 1040–1047. IEEE (2023)
25. Qadri, M., Manchester, Z., Kaess, M.: Learning covariances for estimation with constrained bilevel optimization. In: 2024 IEEE International Conference on Robotics and Automation (ICRA). pp. 15951–15957. IEEE (2024)
26. Qadri, M., Sodhi, P., Mangelson, J.G., Dellaert, F., Kaess, M.: Incopt: Incremental constrained optimization using the bayes tree. In: 2022 IEEE/RSJ International Conference on Intelligent Robots and Systems (IROS). pp. 6381–6388. IEEE (2022)
27. Qadri, M., Zhang, K., Hinduja, A., Kaess, M., Pediredla, A., Metzler, C.A.: Aoneus: A neural rendering framework for acoustic-optical sensor fusion. In: ACM SIGGRAPH 2024 Conference Papers. pp. 1–12 (2024)
28. Qiu, L., Chen, G., Gu, X., Zuo, Q., Xu, M., Wu, Y., Yuan, W., Dong, Z., Bo, L., Han, X.: Richdreamer: A generalizable normal-depth diffusion model for detail richness in text-to-3d. In: Proceedings of the IEEE/CVF conference on computer vision and pattern recognition. pp. 9914–9925 (2024)
29. Qu, Z., Vengurlekar, O., Qadri, M., Zhang, K., Kaess, M., Metzler, C., Jayasuriya, S., Pediredla, A.: Z-splat: Z-axis gaussian splatting for camera-sonar fusion. IEEE transactions on pattern analysis and machine intelligence **47**(9), 7255–7267 (2024)
30. Rafidashti, M., Lan, J., Fatemi, M., Fu, J., Hammarstrand, L., Svensson, L.: Neuradar: Neural radiance fields for automotive radar point clouds. In: Proceedings of the Computer Vision and Pattern Recognition Conference. pp. 2488–2498 (2025)
31. Ravi, N., Reizenstein, J., Novotny, D., Gordon, T., Lo, W.Y., Johnson, J., Gkioxari, G.: Accelerating 3d deep learning with pytorch3d. arXiv:2007.08501 (2020)
32. Rombach, R., Blattmann, A., Lorenz, D., Esser, P., Ommer, B.: High-resolution image synthesis with latent diffusion models. In: Proceedings of the IEEE/CVF Conference on Computer Vision and Pattern Recognition (CVPR). pp. 10684–10695 (June 2022)
33. Ronneberger, O., Fischer, P., Brox, T.: U-net: Convolutional networks for biomedical image segmentation. In: Navab, N., Hornegger, J., Wells, W.M., Frangi, A.F.

(eds.) Medical Image Computing and Computer-Assisted Intervention – MICCAI 2015. pp. 234–241. Springer International Publishing, Cham (2015)
34. Schaefer, S., Galvis, J.D., Zuo, X., Leutengger, S.: Sc-diff: 3d shape completion with latent diffusion models. arXiv preprint arXiv:2403.12470 (2024)
35. Shen, T., Gao, J., Yin, K., Liu, M.Y., Fidler, S.: Deep marching tetrahedra: a hybrid representation for high-resolution 3d shape synthesis. In: Advances in Neural Information Processing Systems (NeurIPS) (2021)
36. Si, Z., Yuan, W.: Taxim: An example-based simulation model for gelsight tactile sensors. IEEE Robotics and Automation Letters **7**(2), 2361–2368 (2022). https://doi.org/10.1109/LRA.2022.3142412
37. Suresh, S., Qi, H., Wu, T., Fan, T., Pineda, L., Lambeta, M., Malik, J., Kalakrishnan, M., Calandra, R., Kaess, M., et al.: Neuralfeels with neural fields: Visuotactile perception for in-hand manipulation. Science Robotics **9**(96), eadl0628 (2024)
38. Suresh, S., Si, Z., Mangelson, J.G., Yuan, W., Kaess, M.: Shapemap 3-d: Efficient shape mapping through dense touch and vision. In: 2022 International Conference on Robotics and Automation (ICRA). pp. 7073–7080. IEEE (2022)
39. Swann, A., Strong, M., Do, W.K., Camps, G.S., Schwager, M., Kennedy, M.: Touch-gs: Visual-tactile supervised 3d gaussian splatting. In: 2024 IEEE/RSJ International Conference on Intelligent Robots and Systems (IROS). pp. 10511–10518. IEEE (2024)
40. Wang, G., Chen, Z., Loy, C.C., Liu, Z.: Sparsenerf: Distilling depth ranking for few-shot novel view synthesis. In: Proceedings of the IEEE/CVF international conference on computer vision. pp. 9065–9076 (2023)
41. Wang, P., Liu, L., Liu, Y., Theobalt, C., Komura, T., Wang, W.: Neus: learning neural implicit surfaces by volume rendering for multi-view reconstruction. In: Proceedings of the 35th International Conference on Neural Information Processing Systems. NIPS '21, Curran Associates Inc., Red Hook, NY, USA (2021)
42. Wang, S., She, Y., Romero, B., Adelson, E.: Gelsight wedge: Measuring high-resolution 3d contact geometry with a compact robot finger. In: 2021 IEEE International Conference on Robotics and Automation (ICRA). pp. 6468–6475 (2021). https://doi.org/10.1109/ICRA48506.2021.9560783
43. Wang, Y., Zhang, Z., Qiu, J., Sun, D., Meng, Z., Wei, X., Yang, X.: Touch2shape: Touch-conditioned 3d diffusion for shape exploration and reconstruction. In: Proceedings of the Computer Vision and Pattern Recognition Conference. pp. 5656–5665 (2025)
44. Wang, Z., Lu, C., Wang, Y., Bao, F., Li, C., Su, H., Zhu, J.: Prolificdreamer: High-fidelity and diverse text-to-3d generation with variational score distillation. Advances in neural information processing systems **36**, 8406–8441 (2023)
45. Wu, R., Mildenhall, B., Henzler, P., Park, K., Gao, R., Watson, D., Srinivasan, P.P., Verbin, D., Barron, J.T., Poole, B., et al.: Reconfusion: 3d reconstruction with diffusion priors. In: Proceedings of the IEEE/CVF conference on computer vision and pattern recognition. pp. 21551–21561 (2024)
46. Yuan, W., Khot, T., Held, D., Mertz, C., Hebert, M.: Pcn: Point completion network. In: 2018 international conference on 3D vision (3DV). pp. 728–737. IEEE (2018)
47. Yuan, W., Dong, S., Adelson, E.H.: Gelsight: High-resolution robot tactile sensors for estimating geometry and force. Sensors **17**(12), 2762 (2017)
48. Zhang, H., Zhang, X., Huang, J., Feng, Z., Xiao, X.: End-to-end diffusion-based 3d object reconstruction from robotic tactile sensing. IEEE Robotics and Automation Letters **11**(2), 1434–1441 (2025)

49. Zhao, C., Sun, S., Wang, R., Guo, Y., Wan, J.J., Huang, Z., Huang, X., Chen, Y.V., Ren, L.: Tclc-gs: Tightly coupled lidar-camera gaussian splatting for autonomous driving: Supplementary materials. In: European Conference on Computer Vision. pp. 91–106. Springer (2024)
50. Zhou, Q.Y., Park, J., Koltun, V.: Open3D: A modern library for 3D data processing. arXiv:1801.09847 (2018)
51. Zou, Z., Cheng, W., Cao, Y.P., Huang, S.S., Shan, Y., Zhang, S.H.: Sparse3d: Distilling multiview-consistent diffusion for object reconstruction from sparse views. In: Proceedings of the AAAI conference on artificial intelligence. vol. 38, pp. 7900–7908 (2024)